

Wave Boundary Layer: Parameterization Technique and Its Proof

M. BELEVICH*, A. SAFRAY*, KWI-JOO LEE** AND KYOUNG-HWA KIM**

*Wave Research Center, General Physics Institute, Russian Academy of Sciences, Russia

**Department of Naval Architecture and Ocean Engineering, Chosun University, Gwangju, Korea

KEY WORDS: Wave Boundary Layer (WBL), Parameterization Technique, Superposition Principle, Arbitrary Wind Direction, Parameterization of Drag

요 약: 본 논문에서는 바다의 자유표면에서 생성되는 항력에 대한 물리적 특성에 대한 연구가 기술되었다. 2차원 파장(Wave Field) 매개변수해석기법(Parametric Analyzing Technique)을 근거로 한 파경계층(Wave Boundary Layer :WBL)의 1차원 모델로서 항력계산과 파경계층의 특성을 추정하였으며 이론의 간략화(Simplifying)에 대한 연구에 주력하였다.

1. Introduction

The local thermodynamic interaction is an important element of an ocean-atmosphere system. The accuracy of its parameterization determines the quality of climate modeling, weather prediction and ecological forecasting.

The main problem in the theory of the near-surface boundary layer is to establish a relation between turbulent stress T and wind velocity vector u at an arbitrary height

$$T = \rho_a C |u| u \quad (1)$$

where ρ_a is air mass density and C is the drag coefficient. Contrary to the case of the solid lower boundary, which is described by only one morphological characteristic, the roughness parameter z_0 , the sea surface is not predetermined due to waves produced by local wind and swell.

Far from the surface, at heights more than a wave boundary layer specific height h_w , the wave-induced fluctuations attenuate, and in case of stationarity and horizontal homogeneity the boundary layer above the waves is very close to that above a solid flat surface. In particular, the turbulent momentum flux is constant with height and the wind profile is nearly logarithmic.

However, near the waves the role of wave-induced fluctuations increases and immediately above the surface, the resemblance to the usual boundary layer disappears completely. The drag coefficient is formed jointly by all drag

mechanisms arising in the relatively thin layer near the interface.

Existing computational methods for the momentum flux above waves are usually based on simple Charnock's relation $z_0 = m \frac{v_*^2}{g}$, where v_* is the friction velocity, m is an empirical coefficient and g is the gravity acceleration. Although this expression gives a good scale for the roughness parameter, it may be considered as a qualitative estimate since it does not take into account the specific character of a given wave field. Using Charnock's relation, the drag law may be written as follows

$$\ln \frac{|u|^2}{gz} = -\ln(mC) - \frac{k}{\sqrt{C}} \quad (2)$$

which connects the drag coefficient C with the wind velocity at any height z . It has been noted in(Chalikov and Belevich, 1993) that this expression gives a rather weak dependence of C on wind velocity since it is assumed that the wind and waves are adapted to each other and that the wave field is fully developed. Often, this is not correct because the space and time scales of a stationary wave field under a sufficiently strong wind are too large. As a result, in a general case, the drag coefficient depends not only on the wind velocity, but also on the 2D wave spectrum $S(Vk)$

$$C = C \left(\frac{|u|^2}{gz}, S(Vk) \right) \quad (3)$$

This problem has been considered in Chalikov(1993). Using the 1D model of the boundary layer above waves an

approximate formula which binds the drag C with wind velocity and wave age has been developed. However, some simplifying assumptions have been made. They are as follows:

- angular wave distribution is considered to be symmetric with respect to the wind direction.
- non-linear inter-mode interactions are regarded small and are neglected.
- stratification is assumed to be neutral.

In the recent papers (Belevich, 1996, Belevich, 2000) it has been shown that the last two assumptions are quite possible and in regular meteorological situations do not generate serious errors. The first assumption has not been analysed yet. We present such analysis here and summarize all the work done in connection with the problem of parameterization of the wave boundary layer. This is the objective of our study.

The paper is organized as follows. In Section 2 a 1D model of WBL is introduced. Section 3 is devoted to describing parameterization of drag under a 2D wave field. Estimation of simplifying assumptions of the model is presented in Section 4.

2. 1D Model of the Wave Boundary Layer

Surface wind waves generate a specific wave boundary layer (WBL) whose properties differ from those of the surface mixed layer. Main difference between the WBL and the boundary layer over a fixed flat surface consists in an onset of an additional momentum flux due to wave fluctuations of pressure, velocity and turbulent stress. Since the momentum balance takes place in a stationary WBL the wave-induced momentum flux causes variations of the turbulent momentum flux and deviations in the wind velocity profile from the logarithmic one inside the WBL and additive changes of wind velocity outside the WBL. Within the logarithmic interval of the wind profile it is convenient to describe these effects using the so-called total roughness parameter which takes into account the wave drag of both parts of the wave spectrum, i.e. low-frequency part and the universal range where Phillips' law is assumed. One of the main objectives of the work is elaboration of a computational algorithm for the WBL structure above an arbitrary wave field, including waves produced by non-local wind, i.e. swell.

The structure of the stationary WBL is governed by the momentum balance equation

$$\partial_{\zeta}(T + \tau) = 0 \quad (4)$$

where T and τ are the vertical components of the turbulent stress and the wave induced stress (or wave induced momentum flux), respectively, ζ is the vertical coordinate the origin of which is located on the wave surface.

Assuming that $T = K\partial_{\zeta}u$, where K is the turbulent viscosity coefficient and u is the horizontal wind velocity, we obtain

$$\partial_{\zeta}(K\partial_{\zeta}u + \tau) = 0 \quad (5)$$

The upper boundary of the WBL is defined by conditions

$$T|_{h_w} = T_h, \quad \tau|_{h_w} = 0 \quad (6)$$

Integration of (5) within (ζ, h_w) , gives

$$K\partial_{\zeta}u + \tau = T_h \quad (7)$$

The unknown coefficient K in equation (7) may be expressed in terms of turbulent energy density e and the so-called mixing length ℓ

$$K = \ell \sqrt{\frac{e}{c_1}} \quad (8)$$

Here $c_1 \approx 4.6$ is an empirical constant. To calculate the scale ℓ the simplest hypothesis is used $\ell \approx \alpha \zeta$. The turbulent energy density e is computed using the turbulent energy balance equation

$$P + \partial_{\zeta}K\partial_{\zeta}e - \frac{1}{\ell} \left(\frac{e}{c_1} \right)^{\frac{3}{2}} = 0 \quad (9)$$

The second and third terms describe the diffusion and dissipation of e , respectively. The first term is production of the turbulent energy via the velocity shift and may be taken in the form (see discussion in Chalikov(1993))

$$P = (K\partial_{\zeta}u + \tau)\partial_{\zeta}u = T_h\partial_{\zeta}u \quad (10)$$

The equation (9) now takes the form

$$T_h\partial_{\zeta}u + \partial_{\zeta}K\partial_{\zeta}e - \frac{1}{\ell} \left(\frac{e}{c_1} \right)^{\frac{3}{2}} = 0 \quad (11)$$

Using the scales v_*^2/g for length and v_*^2/g for time, where v_* is treated as $\sqrt{|T_h|/\rho_a}$ we rewrite the system of equations (7), (11) in non-dimensional form (non-dimensional variables are marked by the tilde)

$$\tilde{K}d_{\tilde{\zeta}}\tilde{u}=1-\tilde{\tau} \quad (12)$$

$$d_{\tilde{\zeta}}u+d_{\tilde{\zeta}}\tilde{K}d_{\tilde{\zeta}}\tilde{e}-\frac{1}{\tilde{K}}\left(\frac{\tilde{e}}{c_1}\right)^2=0 \quad (13)$$

The boundary conditions are as follows

$$\tilde{e}=c_1, \quad \tilde{\zeta}=\tilde{h}_w \quad (14)$$

$$d_{\tilde{\zeta}}\tilde{e}=0, \quad \tilde{\zeta}=0 \quad (15)$$

$$\tilde{K}d_{\tilde{\zeta}}\tilde{u}=C_r|\tilde{u}_r|\tilde{u}_r, \quad \tilde{\zeta}=\tilde{\zeta}_r \quad (16)$$

Here \tilde{u}_r and C_r are the wind velocity and the local drag coefficient at the height $\tilde{\zeta}_r$, respectively, and $\tilde{\zeta}_r$ is small enough height lying in the interval $\left(\frac{2\pi}{\tilde{\omega}_2^2}, \frac{2\pi}{\tilde{\omega}_1^2}\right)$, where $(\tilde{\omega}_1, \tilde{\omega}_2)$ is the frequency band which includes Phillips' spectrum

$$\tilde{S}(\tilde{\omega})=a\tilde{\omega}^{-5}, \quad a=const \quad (17)$$

The first boundary condition implies that \tilde{e} is constant above the wave boundary layer. The second one means that at a small height $\tilde{\zeta}=\tilde{\zeta}_r$, dissipation of \tilde{e} is balanced by its production. The necessity to choose lower boundary condition at height $\tilde{\zeta}_r$ is discussed in Chalikov(1993) in details.

Vertical component of the wave-induced momentum flux $\tilde{\tau}$ is computed using the technique suggested in Chalikov (1993). Neglecting the non-linear effects it is possible to write the flux τ over an arbitrary wave field as a superposition of the "elementary" wave fluxes $F(\omega)$, which are induced independently by each spectral component:

$$\tau(\zeta)=\rho_w g \int_0^{\omega_r} F(\omega)f(\zeta)d\omega \quad (18)$$

where ρ_w is the water mass density, ω_r is the frequency which corresponds to the wavelength ζ_r , and $f(\zeta)$ is the vertical distribution function. The results of numerical

experiments with 2D WBL model Makin(1996) allowed suggestion of the approximate formula for the vertical distribution of the momentum flux τ induced by the monochromatic wave Chalikov(1993):

$$f(\zeta)\equiv\frac{\tau}{\tau_0}=\left(1-\frac{\zeta}{\xi_0}\right)\cdot e^{-10\zeta/\lambda} \quad (19)$$

$$\xi_0=\frac{\zeta}{\lambda} \quad \xi_0=0.31-50C_\lambda$$

where τ_0 is the surface value of the momentum flux, $\lambda=\frac{2\pi g}{\omega^2}$ is the wave length, and C_λ is the value of drag coefficient on the height $\zeta=\lambda$. Thus, the disturbances induced by wave decreases in e times on the height ζ of the order of 0.1λ . Since the presence of a strongly pronounced maximum on the peak frequency ω_p and sharp decaying in the neighbouring low frequency domain are typical features of the developing waves, it is quite natural to define the height of the WBL as the value which is proportional to the wave length of the peak frequency, namely:

$$h_w \approx 0.1 \frac{2\pi g}{\omega_p^2} \quad (20)$$

The flux $F(\omega)$ which corresponds to the 2D wave spectrum $S(k)=S(\omega)D(\omega, \theta)$, where $S(\omega)$ is the frequency spectrum and $D(\omega, \theta)$ is the angular distribution of the wave field, may be written as follows

$$F(\omega)=\int_{-\pi}^{\pi} kS(\omega)D(\omega, \theta)\beta(\omega, \theta)d\theta \quad (21)$$

Here $k=(k_1, k_2)$ is the wave number, $k_1=\frac{\omega^2}{g}\cos\theta$, $k_2=\frac{\omega^2}{g}\sin\theta$, and the weight function β is the so-called wind-wave interaction (WWI) parameter. The waveward energy flux ε then reads

$$\varepsilon(\omega)=\rho_w \int_{-\pi}^{\pi} \omega S(\omega)D(\omega, \theta)\beta(\omega, \theta)d\theta \quad (22)$$

3. Parameterization of Drag over the 2D Wave Field

The 1D model formulated above has been used to elaborate the parameterization scheme of the WBL over an arbitrary 2D wave field. As an example, two model spectra

have been considered, namely: Pierson-Moscovitz spectrum for developed waves (WAMD Group(Hasselmann, et al, 1988)) and JONSWAP spectrum approximation for developing sea waves. Below both spectra are written in terms of relative frequency $o = \frac{\omega}{\omega_p}$.

Pierson-Moscovitz spectrum:

$$S_{PM}(\tilde{\omega}) = (\alpha_{PM} \tilde{\omega}_p^{-5}) o^{-5} \exp\left(-\frac{5}{4} o^{-4}\right) \quad (23)$$

where

$$\alpha_{PM} = 0.0081, \quad \tilde{\omega}_{PM} = 0.033 \quad (24)$$

JONSWAP spectrum:

$$S_J(\tilde{\omega}) = (\alpha_J \tilde{\omega}_p^{-5}) o^{-5} \exp\left(-\frac{5}{4} o^{-4}\right) \gamma_J^{G_J} \quad (25)$$

where

$$\alpha_J = 0.57 \tilde{\omega}_p^{1.5}, \quad \gamma_J = 3.3 \quad (26)$$

$$G_J = \exp\left(-\frac{1}{2} \left(\frac{1-o}{\sigma_J}\right)^2\right)$$

$$\sigma_J = \begin{cases} 0.07, & o \leq 1, \\ 0.09, & o \geq 1. \end{cases} \quad (27)$$

The directional distribution for both spectra was taken in JONSWAP form:

$$D_J(\tilde{\omega}, \theta) = N_s^{-1} \cos^{2s}\left(\frac{\theta}{2}\right) \quad (28)$$

where

$$N_s = \int_{-\pi}^{\pi} \cos^{2s}\left(\frac{\theta}{2}\right) d\theta = 2\sqrt{\pi} \frac{\Gamma(s + \frac{1}{2})}{\Gamma(s + 1)} \quad (29)$$

$$s = 9.77 o^\mu, \quad \mu = \begin{cases} 4.06, & o \leq 1, \\ -2.34, & o > 1. \end{cases} \quad (30)$$

Here $\Gamma(s)$ is a gamma-function.

Assuming the symmetric angular distribution $D(\tilde{\omega}, \theta)$ with respect to wind direction we let the lateral stress component be equal to zero. Numerical integration of the model equations has been performed for a number of fetches defined by non-dimensional peak frequency $\tilde{\omega}_p$. The following values of $\tilde{\omega}_p$ were used: 0.06, 0.10, 0.15,

0.20. The Pierson-Moscovitz and JONSWAP spectra for different values of $\tilde{\omega}_p$ are shown in Fig. 1a. The specific feature of this model spectrum is a well pronounced overshoot effect. Namely, for any given frequency $\tilde{\omega} > \tilde{\omega}_p$, the smaller the fetch, the greater the value of the spectral energy density $S_J(\tilde{\omega})$. Fig. 1b shows the spectral density distribution of the energy flux computed according to Equation (22). The density of the energy flux increases with increasing fetch, and its maximum is located in the vicinity of the peak frequency. The spectral density of the momentum flux (see Fig. 1c) computed according to Equation (21) shows an inverse regularity: its maximum decreases with increasing fetch mainly due to the overshoot effect.

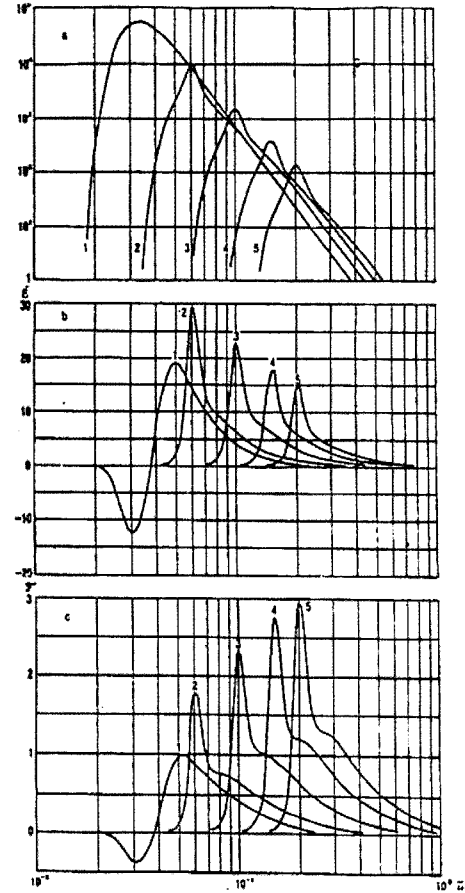


Fig. 1 (a) Wave spectra $\tilde{S}(\tilde{\omega})$; (b) Wave energy flux density $\tilde{\varepsilon}(\tilde{\omega})$; (c) Wave momentum flux density for different wave ages: 1 - $\tilde{\omega}_p = 0.033$ (Pierson-Moscovitz spectrum), 2 - $\tilde{\omega}_p = 0.06$, 3 - $\tilde{\omega}_p = 0.10$, 4 - $\tilde{\omega}_p = 0.15$, 5 - $\tilde{\omega}_p = 0.20$ (JONSWAP spectrum)

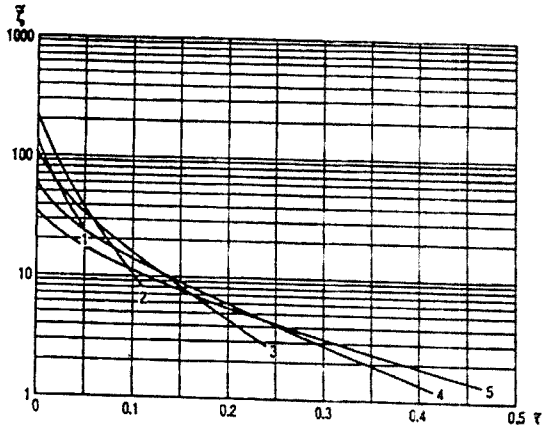


Fig. 2 Vertical distribution of momentum flux τ for different wave ages. Captions as in Fig. 1

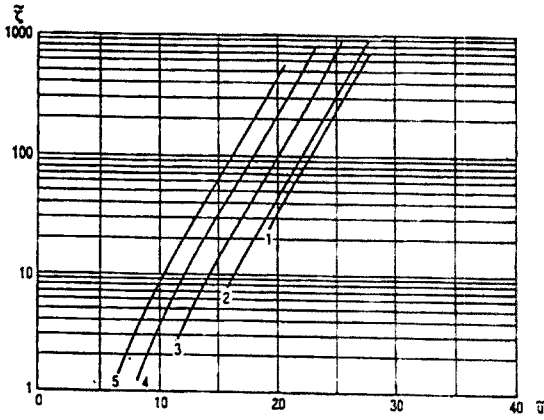


Fig. 3 Vertical profiles of wind velocity $|\tilde{u}|$ for different wave ages. Captions as in Fig. 1

The vertical profiles of the wave-produced momentum flux computed using (18) are shown in Fig. 2. The larger the fetch, the smaller the flux, but the greater the height because it is produced by longer waves. In spite of the rapid vertical attenuation of the wave-induced flux of momentum with small fetches, the drag effects are stronger than with large fetches. This phenomenon may be explained using the simplified equation of turbulent energy balance. Neglecting the diffusion it is possible to obtain the solution

$$\tilde{u} = \frac{1}{\sqrt{C}} = \frac{1}{\alpha} \int_{\tilde{z}_0}^{\tilde{z}} \frac{(1 - \tilde{\tau})^{\frac{3}{4}}}{\tilde{\zeta}} d\tilde{\zeta} \quad (31)$$

Showing that the drag coefficient depends monotonically on the integral of the wave-induced momentum with respect

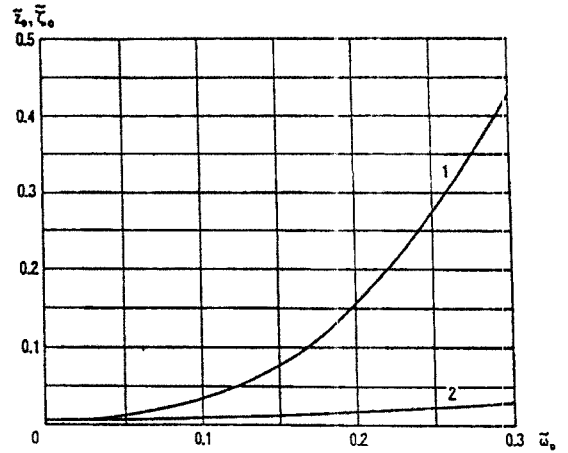


Fig. 4 Dependence of roughness on peak frequency \tilde{w}_p : 1- total roughness parameter \tilde{z}_0 (numerical solution). 2- local roughness parameter $\tilde{\zeta}_0$ in accordance with(33)

to height.

Although $\tilde{\tau}$ at small heights may be sufficiently large, the wind profiles (Fig. 3) are nearly logarithmic and shifted due to variations of the total roughness parameter. Thus, except for a thin layer in the vicinity of the wave surface, the following expression,

$$\tilde{z}_0 = \tilde{z}, e^{-\alpha \tilde{u}} \quad (32)$$

gives in practice, the same values of the total roughness parameter.

The dependence of \tilde{z}_0 and $\tilde{\zeta}_0$ on \tilde{w}_p is shown in Fig. 4. The values of $\tilde{\zeta}_0$ have been calculated using the formula (see (Chalikov and Belevich, 1993))

$$\tilde{\zeta}_0 = 0.075 \tilde{w}_p^{\frac{3}{4}} \quad (33)$$

Significant variations of $\tilde{\zeta}_0$ with respect to peak frequency (or wave age) demonstrate the important role of the wave-induced drag.

The relation of the drag law type

$$C = C\left(\frac{u^2}{g\tilde{\zeta}}, \tilde{w}_p\right) \quad (34)$$

is a convenient characteristic of the wave boundary layer. This function was calculated using the solution of the problem (13)-(16) and is shown in Fig. 5b. Relation (2),

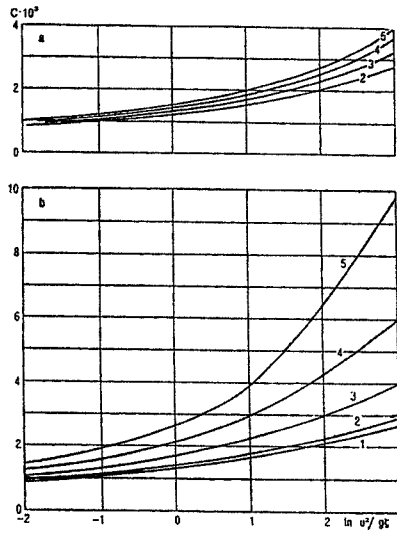


Fig. 5 Dependence of drag coefficient $C(z)$ on $\ln(|u(z)|^2/gz)$: (a) ζ_0 depends on \tilde{w}_p only; (b) numerical solution. Captions as in Fig. 1

with non-dimensional local roughness parameter m equal to ζ_0 is plotted in Fig. 5a for comparison. This formula gives a weaker dependence of C on both arguments. Hence, the drag over the sea surface is formed by the specific wave situation rather than the high-frequency universal part of the spectrum.

Using data in Fig. 5b, it is possible to derive a drag law which connects the drag coefficient at any arbitrary height ζ with external parameters $R = \ln(u^2/g\zeta)$ and $\Omega = u/c_p$ (where u is the wind velocity at height ζ). This dependence may be approximated by the relation

$$\begin{aligned} \ln C = & -6.460 + 0.102\Omega + 0.009\Omega^2 \\ & + (0.311 + 0.055\Omega + 0.006\Omega^2)R \\ & + (0.032 + 0.011\Omega + 0.001\Omega^2)R^2 \end{aligned}$$

4. Study of Simplifying Assumptions

The parameterization described has been developed using some simplifying assumptions, namely:

1. stratification has been assumed to be neutral,
2. non-linear inter-mode interactions have been regarded small and neglected,
3. angular wave distribution has been considered to be symmetric with respect to the wind direction.

We have considered the possibility of these assumptions and below are summarized the corresponding results.

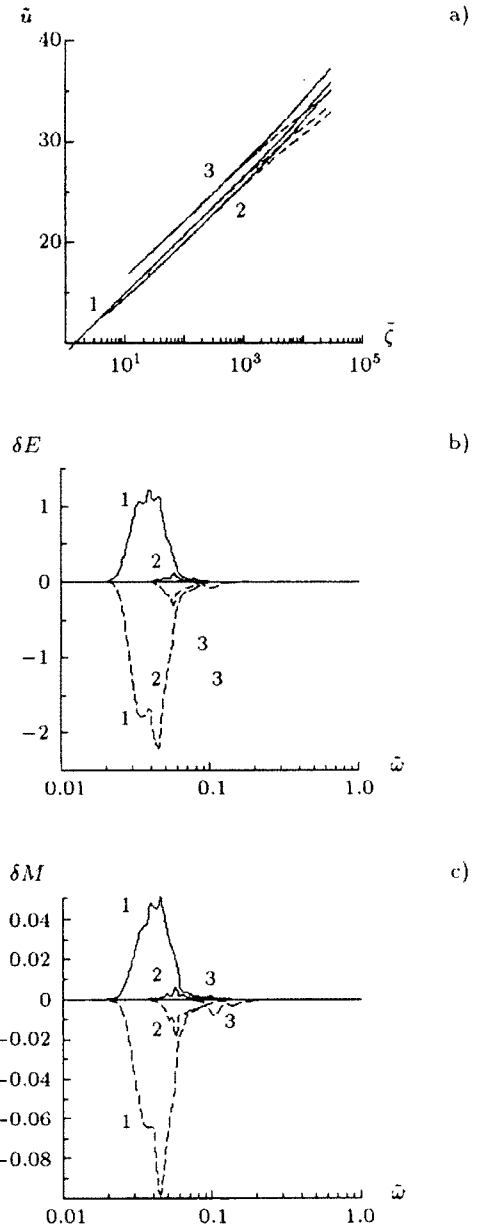


Fig. 6 Influence of air stratification on the WBL characteristics: (a) wind velocity; (b) deviation of the wave energy flux density $\delta\tilde{\varepsilon}(\tilde{w})$; (c) wave momentum flux density $\delta\tilde{F}(\tilde{w})$ with respect to the neutral stratification for different wave ages :

- 1 - $\tilde{w}_p = 0.033$ (Pierson-Moscovitz spectrum), 2 - $\tilde{w}_p = 0.06$,
- 3 - $\tilde{w}_p = 0.10$, (JONSWAP spectrum). Solid line - $\tilde{T}_* = 0.5 \cdot 10^{-3}$, dash line - $\tilde{T}_* = -1.0 \cdot 10^{-3}$

4.1 Arbitrary Stratification of WBL

The overwhelming majority of investigations concerning the boundary layer above waves regards the air within the WBL to be neutrally stratified. To what extent this assumption is limiting? Qualitative as well as quantitative estimates have been produced in (Belevich, 1996).

Wind profiles in a stratified boundary layer differ from the logarithmic profile and following (Monin and Yaglom, 1971), may be described using the universal function ψ of the non-dimensional argument σ :

$$u = \frac{v_*}{\kappa} (\psi(\sigma) - \psi(\sigma_0))$$

$$\sigma = \frac{z}{L_*}, \quad \sigma_0 = \frac{z_0}{L_*}$$

where v_* is friction velocity, $\kappa = 0.4$ is von Karman's constant and L_* is the so-called Monin-Obukhov length scale.

$$L_* = - \frac{v_*^3 c_p \rho_a}{\kappa b q}$$

Here $b = g/\bar{T}$ is the buoyancy parameter, \bar{T} is the air mean temperature, q is the turbulent heat flux and c_p is the heat capacity of the air. Absolute value and sign of σ characterize the hydrostatic stability of the medium: the stratification is stable when $\sigma > 0$; neutral when $\sigma = 0$, and unstable when $\sigma < 0$. There are a number of approximate formulas for the function ψ , which differ from each other mainly by values of the constants. The formula which has been derived in [17], was used in the current research:

$$\ln \sigma + 10 \cdot \sigma, \quad \sigma > 0$$

$$\psi(\sigma) = \ln |\sigma|, \quad \sigma \in [-0.07, 0]$$

$$0.25 + 1.2\sigma^{-\frac{1}{3}}, \quad \sigma < -0.07$$

This function is close to logarithmic for small values of σ and differs from the latter either for large values of $|L_*|$ (heavily stratified medium) or for large heights z .

The ratio of the WBL height h_w to the length scale L_* characterizes the influence of thermal stratification on the WBL structure. In case the stratification is not too far from the neutral ($L_* \in [-10^2, 10^2]$), the order of magnitude of this ratio is near 0.1 even for developed sea. Therefore we may expect that the influence of stratification is insignificant for small fetches, increases with developing waves and becomes apparent mainly in the low-frequency part of the spectrum.

The quantitative estimates may be obtained using a modified 1D WBL model. The modification is involved in taking into account mutual transformations of turbulent and potential energies of the liquid column with variable mass

density in the gravity field

$$b \frac{q}{c_p \rho_a} = - \frac{v_*^3}{\kappa L_*} = - \kappa v_* b T_*$$

where T_* is temperature scale which is connected with the length scale L_* via the relation

$$L_* T_* = \frac{v_*^2}{\kappa^{2b}}$$

Using the modification described, the turbulent energy balance equation (13) is now written as follows

$$d_{\xi} u + d_{\xi} \tilde{K} d_{\xi} \tilde{e} - \frac{1}{\tilde{K}} \left(\frac{\tilde{e}}{c_1} \right)^2 - \chi \tilde{T}_* = 0$$

where $\tilde{T}_* = T_*/\bar{T}$, $\tilde{T}_* = (\kappa^2 \tilde{L}_*)^{-1}$, $\tilde{L}_* = g L_* / v_*^2$.

This new problem has been solved for various wave situations and the values of \tilde{T}_* within the range $[-10^{-3}, 10^{-3}]$. The developed sea has been simulated via the Pierson-Moscovitz spectrum (23); in case of developing seas the JONSWAP spectrum (25) with $\tilde{\omega}_p = 0.06; 0.1$ has been used.

Calculations done verify the above-made qualitative considerations. Wind profiles for non-neutral stratifications (see Fig. 6a) coincide with the logarithmic profile for small heights and noticeably differ from it near the upper border of the computational domain. The stratification influences significantly upon the energy and momentum exchange (see Fig. 6b and 6c, respectively) in case of developed sea only when the main energy-bearing part of the spectrum is located in the low-frequency domain. In all other cases the influence of stratification is negligibly small. Thus, not taking into the account the heavily stratified air the wave boundary layer over developing waves may be considered to a first approximation neutrally stratified and the above-produced parameterization scheme may be used without modification.

It is worth mentioning that the results obtained may be used in more general situation of the mass density stratification. In this case the scales L_* and T_* should be changed to L^* and T^* , respectively:

$$L^* = L_* \left(1 + \frac{0.075}{Bo} \right)^{-1}, \quad T^* = T_* \left(1 + \frac{0.075}{Bo} \right) \quad (35)$$

where Bo is the Bowen ratio. For small values of Bo the

influence of the humidity stratification becomes comparable with the effects of the thermal stratification. In this case the non-dimensional correction term in (35) is close to unity and must not be neglected.

4.2 Superposition Principle

In (Belevich and Neelov, 2000) the mutual influence of the wave components on the energy interchange with the wave boundary layer has been estimated. In case this influence is negligible, the superposition principle which plays an important role in the whole theory is applicable.

The 1D model of the wave boundary layer described above has been used in a study of the air flow over a two-mode wave surface. The Low Frequency (LF) mode $\tilde{\omega}_L$ changed within the interval (0.06, 0.4). The values of the High Frequency (HF) mode $\tilde{\omega}_H$ were calculated using the dispersion relation for high frequency wave number k_H divisible by low frequency wave number k_L with the factor equal to 2^n , $n=1, \dots, 5$. Amplitudes a of the wave modes have been chosen using the condition $ak=0.1$. Note that according to (Makin, 1983) and our calculations the dependence of the wind-wave interaction on the wave steepness ak for the values within the range [0.05, 0.3] is nearly absent.

Evaluation of mutual influence of the wave components on the energy interchange with the WBL has been carried out in terms of the wind-wave interaction parameter $\beta(\omega)$. Values of the function β calculated for the two-mode surface have been compared with those of this function β_0 for single-mode surface. All numerical experiments undertaken for various values of the wave parameters, using the 3D model of the WBL (Belevich and Neelov, 1998), demonstrate weak mutual influence on the energy exchange. Values of the function $\beta_H = \beta(\omega_H)$ coincide with those of β_0 (see Fig. 7a). Differences $\Delta\beta_H = \beta_H - \beta_0$ are insignificant for all frequencies (see Fig. 7b). Relative variations of the WWI parameter $\delta\beta_H = \Delta\beta_H / \beta_0$ oscillate within the $\pm 30\%$ limits for low frequencies (i.e. for small values of β) and decrease with increasing ω_H .

The influence of the HF mode on the energy exchange of the LF wave component is also weak. Fig. 8a shows that the dependence of $\beta_L = \beta(\omega_L)$ on the frequency of the HF oscillation noticeably differs from the constant for small values of ω_L only, i.e. when $|\beta|$ is small. The calculated differences $\Delta\beta_L = \beta_L - \beta_0$ demonstrate that the presence of the HF mode manifests itself in an insignificant decrease of

the parameter β_L (see Fig. 8b). However, the relative decrease of the WWI parameter $\delta\beta_L = \Delta\beta_L / \beta_0$ do not exceed 5%.

Though the results obtained indicate the existence of mutual influence of the wave components on the energy exchange with WBL, relative variations of the WWI parameter, produced by the non-linear mode interaction are much smaller than the empirical data scatter. Thus, according to (Pierson and Moskowitz, 1964) the estimations of the parameter β differ by a factor of 2-3 for $\omega \sim 1$, and by an order of magnitude for $\omega \sim 0.1$. The same scatter of the WWI parameter values gives various approximate formulas (see Table 3 in (Burgers and Makin, 1993) for reference). Moreover, the numerical values of the WWI parameter obviously depend on the parameterization scheme for turbulent drag, vertical and horizontal resolution used in the numerical model, etc.

Summarizing all that has been said it is possible to conclude that to a first approximation the mutual influence of the wave components may be neglected. Thus, the superposition principle may be considered to be satisfied, and the function $\beta(\omega)$ obtained using the numerical experiments with the air flow over the single-mode surface may be used for calculations of the momentum and energy fluxes.

4.3 Arbitrary Wind Direction

The general non-symmetric case of angular wave distribution with respect to the wind direction is considered. In terms of the WWI parameter this means that the symmetry axes of the 2D $\beta(\tilde{\omega}, \theta)$ parameter distribution and the spatial wave distribution $D(\tilde{\omega}, \theta)$ are directed at an angle ϕ with respect to each other. In order to figure out how erroneous the previous assumption ($\phi=0$) is, a number of numerical experiments with the 1D WBL model have been carried out. The model has been modified to take into account an arbitrary angle ϕ . Namely, the wave-induced momentum flux is now the function of two arguments

$$\tau(\zeta, \phi) = \rho_{\text{veg}} \int_0^{\omega_r} F(\omega, \phi) f(\zeta) d\omega \quad (36)$$

where

$$F(\omega, \phi) = \int_{-\pi}^{\pi} kS(\omega) D(\omega, \theta) \beta(\omega, \theta - \phi) d\theta \quad (37)$$

The wave-induced energy flux ε is written, respectively

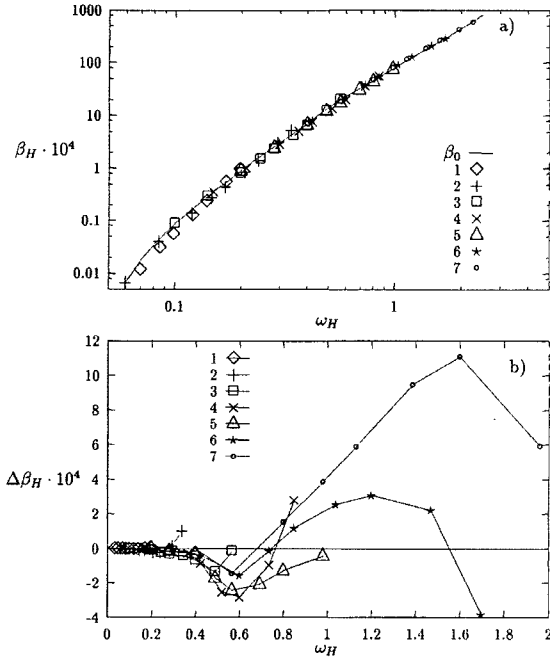


Fig. 7 Dependence of the parameter β_H (a) and the differences $\Delta\beta_H = \beta_H - \beta_0$ (b) on the frequency ω_H for various values of the frequency ω_L : 1) 0.035 ; 2) 0.06 ; 3) 0.1 ; 4) 0.15 ; 5) 0.5 ; 6) 0.3 ; 7) 0.4

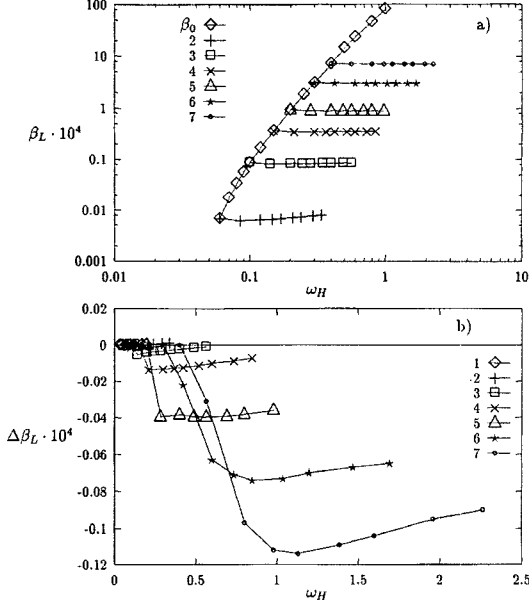


Fig. 8 Dependence of the parameter β_L (a) and the differences $\Delta\beta_L = \beta_L - \beta_0$ (b) on the frequency ω_H for various values of the frequency ω_L : 1) 0.035 ; 2) 0.06 ; 3) 0.1 ; 4) 0.15 ; 5) 0.5 ; 6) 0.3 ; 7) 0.4

$$\varepsilon(\omega, \phi) = \rho_w \int_{-\pi}^{\pi} \omega S(\omega) D(\omega, \theta) \beta(\omega, \theta - \phi) d\theta \quad (38)$$

Fully developed sea has been described via the Pierson-Moscovitz spectrum (23). The developing wave situation has been specified by the known 2D model spectrum JONSWAP (25). Since the Pierson-Moscovitz spectrum is one-dimensional, the JONSWAP angular distributions (28) have been considered in this case. The wind-wave interaction parameter has been calculated using the 2D approximate formulas suggested by Chalikov and Belevich (Chalikov and Belevich, 1993), Makin and Mastenbroek (Makin and Mastenbroek, 1996), and the WAMDI Group (Zaslavsky et al., 1995). All the approximate formulas for the WWI parameter are written below.

Chalikov-Belevich (Chalikov and Belevich, 1993):

$$\beta(\tilde{\omega}, \theta) = 10^{-4}$$

$$-a_1 \tilde{\omega}_a^2 - a_2, \quad \tilde{\omega}_a < -1$$

$$a_3 \tilde{\omega}_a (a_4 \tilde{\omega}_a - a_5) - a_6, \quad \tilde{\omega}_a \in (-1, \frac{1}{2} \Omega_1)$$

$$(a_4 \tilde{\omega}_a - a_5) \tilde{\omega}_a, \quad \tilde{\omega}_a \in (\frac{1}{2} \Omega_1, \Omega_1)$$

$$a_7 \tilde{\omega}_a - a_8, \quad \tilde{\omega}_a \in (\Omega_1, \Omega_2)$$

$$a_9 (\tilde{\omega}_a - 1)^2 + a_{10}, \quad \tilde{\omega}_a > \Omega_2$$

Here $\tilde{\omega}_a = \tilde{\omega} \frac{u_\lambda}{v_*} \cos \theta$, u_λ is the absolute value of the wind speed at the height equal to the "apparent" wave length $\lambda_a = \frac{2\pi v_*^2}{\omega^2 g \cos \theta}$, a_1, \dots, a_{10} and Ω_1, Ω_2 are parameters which depend on the drag coefficient at height $\zeta = \lambda_a$:

$$\Omega_1 = 1.075 + 75 C_\lambda, \quad \Omega_2 = 1.2 + 300 C_\lambda$$

$$a_1 = 0.25 + 395 C_\lambda, \quad a_3 = (a_0 - a_2 - a_1) / (a_0 + a_4 + a_5)$$

$$a_2 = 0.35 + 150 C_\lambda, \quad a_5 = a_4 \Omega_1$$

$$a_4 = 0.30 + 300 C_\lambda, \quad a_6 = a_0 (1 - a_3)$$

$$a_9 = 0.35 + 240 C_\lambda, \quad a_7 = (a_9 (\Omega_2 - 1)^2 + a_{10}) / (\Omega_2 - \Omega_1)$$

$$a_{10} = -0.06 + 470 C_\lambda, \quad a_8 = a_7 \Omega_1$$

$$a_0 = 0.25 a_5^2 / a_4$$

Makin--Mastenbroek (Makin and Mastenbroek 1996):

$$\beta(\tilde{\omega}, \theta) = 16 \frac{\rho_a}{\rho_w} \omega^2 \cos^2 \theta$$

WAMDI Group (Zaslavsky et al., 1995):

$$\beta(\tilde{\omega}, \theta) = \max \left\{ 0.25 \frac{\rho_a}{\rho_w} (28 \tilde{\omega} \cos \theta - 1), 0 \right\} \quad (39)$$

Though different approximations for the WWI parameter have been used, the results obtained are quite close and similar. We illustrate our calculations using the WAM formula (39). The dependence of the drag coefficient C on the angle ϕ between the symmetry axes of the wave angular distribution and the 2D WWI parameter is very weak at any height. The maximum relative change δC of $C(\phi)$ with respect to $C(0)$ decreases with growing fetch, and is approximately proportional to logarithm of the peak frequency $\tilde{\omega}_p$. For example, for the Pierson - Moscovitz spectrum $\delta C < 0.1\%$. In case of developing waves (JONSWAP spectrum) our computation results are summarized in the

Table 1. Computation results of developing waves

$\tilde{\omega}_p$	0.04	0.06	0.15	0.2
δC	<0.5%	<2%	<4%	<5%

This unexpected result, however, has a simple explanation. Note that the wave drag is caused mainly by the high-frequency part of the wave spectrum. These HF wave components have small phase velocities in comparison with wind velocity and act to a great extent as roughness elements of the surface and are indifferent to the wind direction.

This reasoning does not explain the above-written dependence $\delta C(\tilde{\omega}_p)$, yet. The decrease of δC with growing fetch is determined by the JONSWAP wave spectrum model which has been used in the current research. As has been mentioned, the specific feature of this spectrum is the overshoot effect, i.e. an increase of the value of the spectral energy density $S_f(\tilde{\omega})$ with the increase of the peak frequency $\tilde{\omega}_p$, for any given frequency $\tilde{\omega} > \tilde{\omega}_p$. Thus, contribution of the HF wave components to the overall drag decreases with growing wave age.

To verify this supposition, we have repeated the last numerical experiments using another wave spectrum model which contrary to JONSWAP, does not possess the overshoot feature. Such a spectrum has been suggested by Donelan, Hamilton and Hui (Donelan et al., 1985):

$$S_D(\tilde{\omega}) = (\alpha_D \tilde{\omega}_p^{-5}) o^{-4} \exp\left(-\frac{5}{4} o^{-4}\right) \gamma_D^{G_D} \quad (40)$$

where

$$\alpha_D = 0.042 \tilde{\omega}_p^{0.55} \quad (41)$$

$$\gamma_D = \begin{cases} 1.7 & \tilde{\omega}_p \leq 0.0414 \\ 10. + 6 \lg \tilde{\omega}_p & \tilde{\omega}_p > 0.0414 \end{cases}$$

$$G_D = \exp\left(-\frac{1}{2} \left(\frac{1-o}{\sigma_D}\right)^2\right) \quad (42)$$

$$\sigma_D = 0.08(1 + 3 \cdot 10^{-4} \tilde{\omega}_p^{-3})$$

The wave angular distribution function is as follows:

$$D_D(\tilde{\omega}, \theta) = \frac{1}{2} q \sec^2 h^2(q\theta)$$

where

$$q = \begin{cases} 2.61, o^{1.3}, & o \in (0.56, 0.95) \\ 2.28, o^{-1.3}, & o \in (0.95, 1.6) \\ 1.24, & \text{otherwise} \end{cases}$$

Indeed, the fetch dependence of the δC has disappeared with a change of the spectrum model. For the spectrum of Donelan et al. the value of δC is approximately 7% for any peak frequency.

Anyway, the error introduced by the assumption of $\phi = 0$ is small and may be neglected in the parameterization schemes of the wave boundary layer.

5. Concluding Remarks

It has been shown that the simplifying assumption of the 1D model of WBL and parameterization scheme based on it cannot introduce big mistakes in the values of the drag and fluxes of momentum and energy on the sea-air interface. All of the chain of the energy transfer from wind to waves and currents has been discussed in (Chalikov and Belevich, 1993). Here we can add that for a rough scheme of ocean-atmosphere interaction on the mesoscales in the framework of coupled ocean-atmosphere models and furthermore on the global scales a simpler parameterization on the basis of the model presented can be developed. It may define the drag and fluxes on the ocean-atmosphere interface directly from the main meteorological characteristics at the lowest computational (observational) level in the atmosphere. A similar approach has been demonstrated in the works of Zaslavsky et al. (Zilitinkevich and Chalikov, 1968).

Acknowledgements

This work was supported by a grant No. 2000-2-305-001-2 from Korea Science & Engineering Foundation.

References

- Belevich, M. (1996). "On the Influence of Thermal Stratification on the Structure of the Wave Boundary Layer," *Izv. Atmos. Ocean. Phys.*, Vol 32, pp 397-401 (in Russian).
- Belevich, M. and Neelov, I. (1998). "On the Approximation of the Wind-Wave Interaction Parameter," *Izv. Atmos. Ocean. Phys.*, Vol 34, pp 435-440 (in Russian).
- Belevich, M. and Neelov, I. (2000). "Evaluation of the Mutual Influence of the Wind-Wave Components on the Energy Interchange with the Wave Boundary Layer," *Meteorologiya i Gidrologiya*, No 1, pp 70-78 (in Russian).
- Burgers, G. and Makin, V. (1993). "Boundary-Layer Model Results for Wind-Sea Growth," *J. Phys. Oceanogr.*, Vol 23, pp 372-385.
- Chalikov, D. and Belevich, M. (1993). "One-dimensional Theory of the Wave Boundary Layer," *Bound. Layer Meteorol.*, Vol 63, pp 65-96.
- Donelan, M.A., Hamilton, J. and Hui, W.H. (1985). "Directional Spectra of Wind-Generated Waves," *Phil. Trans. Roy. Soc. London*, Vol A315, pp 509-562.
- Hasselmann, K., Barnett, T.P., Bouws, E., Carlson, H., Cartwright, D.E., Enke, K., Ewing, J.A., Gienapp, H., Hasselmann, D.E., Kruseman, P., Meerburg, P., Muller, Olbers, D.J., Richter, K., Sell, W. and Walden. H. (1973). "Measurements of Wind-Wave Growth and Swell Decay During the Joint Sea Wave Project (JONSWAP)," *Dtsch. Hydr. Z.*, Bd. A8 (12), pp 1-95.
- Hasselmann, D.E., Dunckel, M. and Ewing, J.A. (1973). "Directional Wave Spectra Observed During JONSWAP," *J. Phys. Oceanogr.*, Vol 10, pp 1264-1280.
- Makin, V.K. (1983). "On the Wind Energy Transfer to Surface Gravity Waves," *Okeanologiya*, Vol XXIII, pp 569-574 (in Russian).
- Makin, V. and Chalikov, D. (1983). "Calculation of Momentum and Energy Fluxes going to Developing Waves," *Izv. Atmos. Ocean. Phys.*, Vol 22, pp 1015-1019 (in Russian).
- Makin, V.K. and Mastenbroek, C. (1996). "Impact of Waves on Air-Sea Exchange of Sensible Heat and Momentum," *Bound. Layer Meteorol.*, Vol 79, pp 279-300.
- Monin A.S. and Yaglom, A.M. (1971). *Statistical Fluid Mechanics*, Vol 1, MIT Press, Cambridge.
- Pierson, W.J. and Moskowitz, L. (1964). "A Proposed Spectral Form for Fully-Developed Wind Seas Based on the Similarity Theory of S.A. Kitaigorodskii," *J. Geophys. Res.*, Vol 69, No 24, pp 5181-5190.
- Plant, W.J., Relationship, A. (1982). "Between Wind Stress and Wave Slope," *J. Geophys. Res.*, Vol 87, pp 1961-1967.
- WAMD Group (Hasselmann, S., Greenwood, J.A., Reistad, M., Zambresky, L., and Ewing, J.A.) (1988). "The WAM Model - A Third Generation Ocean Wave Prediction Model," *J. Phys. Oceanogr.*, Vol 18, pp 1775-1810.
- Zaslavsky, M.M., Kabatchenko, I.M., and Matushevsky, G.V. (1995). "Joint Adaptive Model of the Nearwater Wind and Wind Waves," In Davidan, I.N. (ed.) *Research Problems and Mathematical Modeling of the Wind Waves*, Gidrometeoizdat, St. Petersburg (in Russian).
- Zilitinkevich, S.S. and Chalikov, D.V. (1968). "Determination of Universal Profiles of Wind and Temperature in the Near-Earth Atmospheric Layer," *Izv. Atmos. Ocean. Phys.*, Vol 4, pp 294-302 (in Russian).

2001년 12월 24일 원고 접수

2002년 2월 1일 최종 수정본 채택